Electron correlation effects in the spectral momentum density of graphite

M. Vos, A. S. Kheifets, and E. Weigold
Atomic and Molecular Physics Laboratory, Research School of Physical Sciences and Engineering, The Australian National University, Canberra ACT 0200, Australia

F. Aryasetiawan
Joint Research Center for Atom Technology, Angstrom Technology Partnership, 1-1-4 Higashi, Tsukuba, Ibaraki 305, Japan
(Received 24 October 2000; published 2 January 2001)

The spectral function of an annealed evaporated carbon film was measured using a high-energy (e,2e) spectrometer. Interpretation of these data was relatively straightforward due to low levels of multiple scattering. Large lifetime broadening and strong asymmetries were found in the observed line shapes, with tails extending to large binding energies. A conventional band-structure calculation within the frame of the density functional theory failed to describe the observed intensity. However it could be described well using a calculation of the spectral function based on the cumulant expansion to the single-particle Green's function. Neither the theory nor the experiment showed indications of well-defined intrinsic plasmon structures.

DOI: 10.1103/PhysRevB.63.033108 PACS number(s): 71.10.−w, 79.20.Hx

The major approximation that made most of our understanding of solid-state physics possible is the independent electron approximation. Each electron is moving in an average potential formed by the nuclei and the other electrons. This assumption leads to the familiar theory of k-dependent energies of the Bloch functions (band-structure theory). This approach has been very successful in the description of, for example, the peak positions in angular resolved photoemission experiments.

The fact that this assumption works at all is at first somewhat surprising, as the Coulomb energy corresponding to the average electron-electron separation in a solid is of the order of the bandwidth. However, closer studies have shown that the success of the one-particle theory is due to a large extent by a cancellation between exchange and correlation.[1]

It is in principle possible to avoid making the independent particle approximation. The alternative is to use the Green's function theory. In this approach, the many-body effects are contained in the self-energy operator which is nonlocal and energy dependent. Unfortunately, for extended systems the self-energy is rather hard to calculate even for the electron gas. Approximations must be used and the simplest theory that takes into account screening effects is the GW approximation.[2,3] Numerous calculations on a wide range of real systems have shown the fruitfulness of the GW approximation.[4]

The GW approximation is known to give accurate quasiparticle energies but its description of satellite structures is not satisfactory. In alkali metals, for example, photoemission spectra show the presence of multiple-plasmon satellites whereas the GW approximation yields only one at too large energy. This shortcoming of the GW approximation has been resolved by introducing vertex corrections in the form of the cumulant expansion to the Green's function.[5–7] This allowed the inclusion of multiple plasmon creation. As a result the calculated peak positions of the plasmon satellites were found in a much better agreement with the experiment than those predicted by the GW scheme itself.[8,9]

In photoemission experiments one tries to study the consequences of the electron-electron interaction by observing some of its effects on photoemission spectra. These effects include intrinsic plasmons (see, e.g., Ref. 10), lifetime broadening (the imaginary part of the self-energy) (see, e.g., Ref. 11) and shifts in the peak position (the real part of the self-energy) (e.g., Ref. 12). In principle all these effects are contained in the spectral function. However even in the study of the aspects of the spectral function just mentioned, one has to tread very carefully in distinguishing final and initial state effects, multiple-scattering effects and the applicability of the sudden approximation.

Fortunately there is a high-energy approach that is not impeded to the same extent by these problems as low-energy photoemission. In this approach an incoming particle has a binary collision with a target electron. The kinematics of this collision is influenced by the binding energy and momentum of the target electron. In its most familiar implementation (Compton scattering), the incoming particle is a high-energy photon, and its energy is measured after the collision. As only the photon is measured one can, unfortunately, only resolve directly a projection of the target electron momentum.[13] If the direction of the ejected electron is detected in coincidence, one can measure the complete momentum density, and the technique is then referred to as $(\gamma,e\gamma)$ spectroscopy.[14] For metals the effects of electron-electron interactions can then be observed as a reduction to the discontinuity in the momentum density near k_f.[15,16] If one replaces the incoming photon by an electron it becomes possible to measure the incoming and outgoing energies accurately enough to determine, not only the momentum but also the binding energy of the ejected electron. This is the EMS (electron momentum spectroscopy) experiment, i.e., an (e,2e) experiment in the high-energy limit.

In the previous paragraph we used for convenience some single-particle language. For a truly interacting system we cannot talk about the energy and momentum of an individual electron. Therefore it is more precise to say that in an (e,2e) measurement the difference in momentum of the incoming

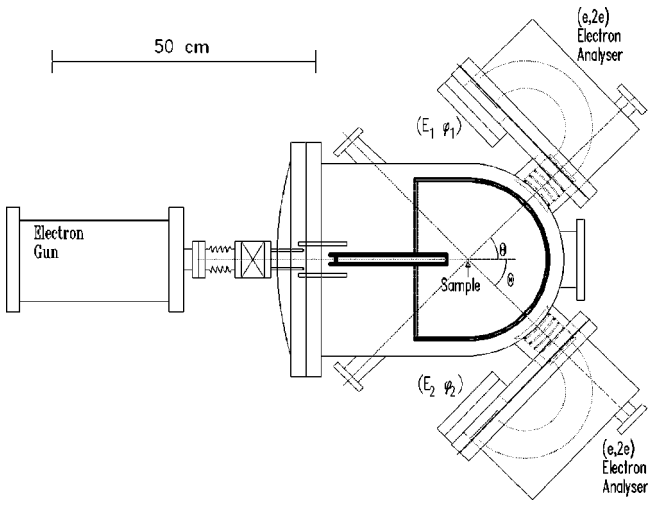

FIG. 1. The outline of the spectrometer. The electron gun produces 25 keV electrons. The dotted lines indicate the positive high voltage area (25 keV). The 50 keV electrons impinge on the sample. The emerging 25 keV electrons are then detected in coincidence in the two electrostatic analyzers (at polar angle $\theta = 44.3°$) that are near ground potential. From each electron the azimuthal angle $\phi_{1,2}$ and energy $E_{1,2}$ are determined from which the separation energy and the target recoil momentum are determined.

particle and the sum of two outgoing particles is the recoil momentum of the ionized system ($\boldsymbol{q}$), and the difference of the kinetic energy of the incoming and the sum of both outgoing electrons is the separation energy (ϵ). The measured intensity $I(\epsilon,\boldsymbol{q})$ can be directly compared to the spectral function, provided that the ionizing event was the only interaction of the incoming and outgoing electrons with the target.[9]

The possibility of measuring the dispersion by EMS is well established,[17–19] and there have been some promising experiments, notably on aluminum,[9] of a more quantitative comparison between these experiments and theory. However the strong interaction of electrons with matter, which makes these experiments feasible with electrons, but currently not with photons, also causes multiple scattering, even for the thinnest self-supporting films ($\simeq$100 Å). Increasing the energy of the incoming and outgoing electrons decreases the level of multiple scattering. For this purpose a spectrometer was constructed, using 50 keV incoming electrons, and detecting outgoing electrons with an energy near 25 keV. Now the thickness of the films can be smaller than the elastic and inelastic mean-free path of the 50 and 25 keV electrons involved. An outline of the spectrometer, which is described in details elsewhere,[20,21] is shown in Fig. 1.

A set of (e,2e) spectra as a function of momentum for the evaporated and subsequently annealed carbon film (nominally 30 Å thick) is shown in Fig. 2. Near zero momentum there is a strong peak at a binding energy of slightly more than 20 eV, which disperses slowly to lower binding energy with increasing momentum. This is the σ-band. The smaller peak that precedes the main component in the momentum range from 0.2 to 0.9 a.u. corresponds to the π-band. The momentum density as obtained from an LDA calculation us-

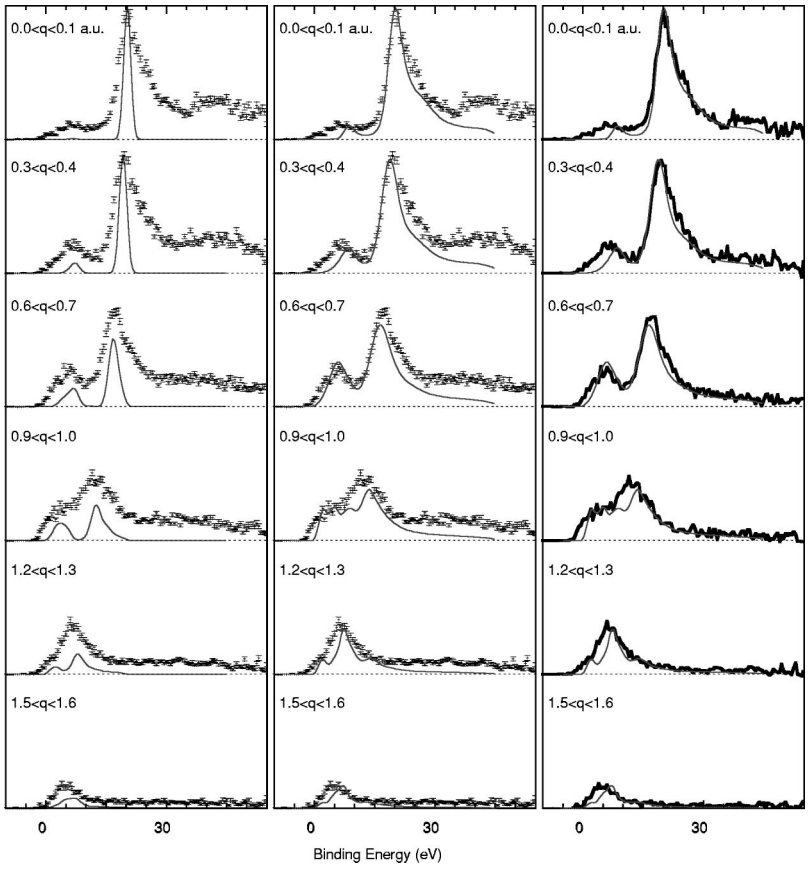

FIG. 2. In the left panel we show the measured (e,2e) spectra (error bars) for selected momentum intervals as indicated, together with the LMTO theory convoluted with the experimental energy and momentum resolution. In the central panel we show the same experimental data, but now compared with the result of a cumulant expansion many-body calculation. Again the theory was broadened with the experimental resolution. In the right panel we show the same theory (thin line) but compare it with the measured intensity after correction for inelastic scattering based on electron energy loss measurements of the same film.

ing the linear muffin-tin orbital (LMTO) method, convoluted with a generous estimate of the experimental resolution (2.0 eV in energy, 0.1 a.u. in momentum), is plotted as well. The measured width of the C 1s core level is 1.8 eV. The calculations are spherically averaged to account for the polycrystalline nature of the specimen. The spectrum at zero momentum was used to scale the maximum height of the theory to that of the experiment. No additional scaling is used for any of the other spectra.

First let us discuss the peak positions. The calculated separation of the π and σ band is somewhat underestimated. This is probably due to the atomic sphere approximation, used in this LMTO calculation. The very open structure of graphite is not well suited for this approach and indeed a full-potential LMTO calculation is known to predict $\simeq 1$ eV larger separation of the σ and π band.[22]

Second, let us focus on the intensity distributions. Whereas the theory predicts only intensity in narrow regions corresponding to the momentum-dependent energies of the π- and σ-band, the experiment shows significant intensity over a much larger energy range. Moreover the shape of the spectra near the bottom of the σ band is asymmetric and much broader than the experimental resolution. The excess width near the bottom of the band is not unusual as the lifetime broadening is largest here. The asymmetry indicates that we cannot describe the data by the result of the LMTO calculation, convoluted with an empirical or theoretical estimate of the lifetime broadening.

This inadequacy of the LMTO method is a general problem of the band-structure methods based on the density functional theory in the LDA form. Therefore we take an alternative approach and perform a full many-body calculation. As in our previous work,[9] we again employ the cumulant expansion scheme. The effects of self-consistency within the cumulant expansion have been investigated for a model electron gas problem.[23] It was found that one iteration was sufficient to reproduce the correct spectral features, and the calculation for graphite was thus restricted to one iteration as well.

As an input to the cumulant expansion scheme we used again the output of an LMTO program that uses the atomic sphere approximation. These calculations are computationally very intensive, and hence the irreducible wedge of the Brillouin zone was covered by a rather sparse grid (54 points only). The spherically averaging was done using a special direction scheme, originally developed for FCC crystals,[24] but adapted for hexagonal structure. Due to the sparseness of the points the averaging was done over five directions only.

The results are shown in the central panel of Fig. 2. Clearly the agreement has improved dramatically. Instead of a sharp peak near zero momentum, as in the LMTO case, we now have a broad asymmetric structure just as in the experiment extending up to 30 eV below the main quasiparticle peak. No clear structures were found in this tail that could be described as an intrinsic plasmon. The height of the σ and π peaks is now close to that found in the experiment over the whole momentum range. The main discrepancy is at high binding energies where the intensity of the measurement exceeds that of the theory. Plasmon excitation by the incoming or outgoing beams, independent of the (e,2e) event (extrinsic plasmons), is the most likely cause of the excess intensity in the experiment.

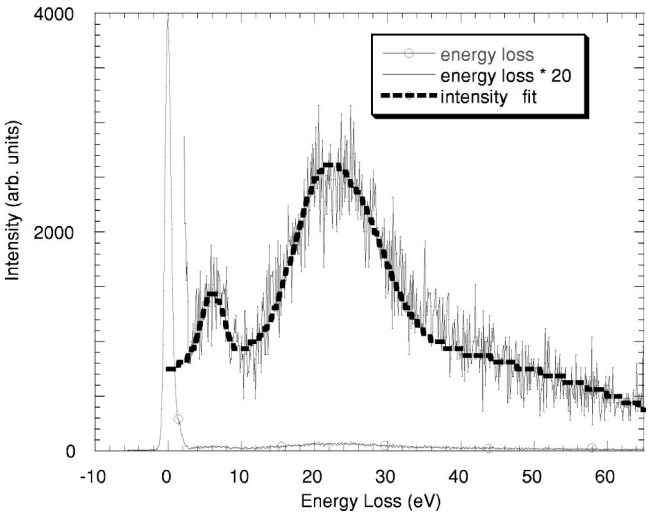

FIG. 3. The energy loss spectrum for 25 keV electrons obtained using one of the two (e,2e) analyzers at the same spot as the actual coincidence measurement. The thick line is a ''fit'' of the energy loss structure used in the deconvolution procedure as described in the text.

In order to establish what level of inelastic scattering one can expect in these experiments we measured an electron energy loss spectrum (EELS) using only one of the two analysers of the spectrometer. The incoming beam was tuned to 25 keV. The result is shown in Fig. 3. Roughly a third of the transmitted electrons suffered energy loss in the film.

The inelastic processes for the incoming and outgoing electrons is rather similar to those in the energy loss measurement, so we can use these spectra to estimate quite accurately how the energy loss processes influence the measured (e,2e) intensity. To do this we consider the trajectories of the 'average' energy loss event and the ''average'' (e,2e) event. As our detector is at approximately 45° all electrons detected in the EELS experiment have been scattered elastically. For the average EELS event the elastic scattering occurred halfway across the film, say at $0.5t$ with t the thickness of the film. The total path length of the trajectory is $0.5t + 0.5t/\sin 45° \simeq 1.2t$. The average (e,2e) event occurs at $0.5t$ as well. However the probability of plasmon excitation by the 50 keV electron is reduced by about a factor of 1.7 (Ref. 25) due to its higher energy. Subsequently there are two electrons emerging, each with path length $0.5t/\sin 45°$. Thus the total effective path length of this average event is $0.5/1.7 + 2 \times 0.5t/\sin 45° \simeq 1.7t$, i.e., about 40% larger than in the EELS case.

The EELS spectrum was fitted, as shown in Fig. 3. The extrinsic loss structure of the (e,2e) event was assumed to be $1.4\times$ higher than that of the EELS measurement, and the corresponding intensity was deconvoluted from the EMS spectra.[26] The results are shown in the right panel of Fig. 2. The agreement with the cumulant expansion calculation is surprisingly good.

Above we deconvoluted the experimental data for inelas-

tic scattering effects. In principle we can also simulate these effects, as well as elastic scattering effects, using Monte Carlo simulations, which take the theoretical spectral function as input.[27] Good agreement can be obtained, but one has to assume the thickness of the film to be considerably larger than the nominal thickness of the film. This applies both to the simulation of the EELS results and the EMS results. Alternatively one has to use a much smaller mean-free path than those quoted in the literature (e.g., Ref. 25).

It is very instructive to compare the result of the LDA theory with those of the cumulant expansion. The peak positions remain virtually constant but in the latter case there is a large intensity away from these peak positions. Thus due to electron-electron correlation the final state can have an energy over a large range (up to 20 eV wide), however the energy at which the maximum occurs is very close to the energy given by a simple band-structure calculations. Thus for a more quantitative analysis of spectra, which does not restrict itself to the peak positions, calculations beyond mean-field theories required. These results are thus a step forward in our program to establish EMS as a tool for truly quantitative studies of the electronic structure of materials. Next we plan to study single-crystal graphite. A comparison with single crystals would avoid the spherical averaging step necessary for polycrystalline samples, and hence will provide an even more critical test of theory. As a number of approximations are made in the presently employed cumulant expansion theory, such a test is particularly desirable.

This spectrometer could not have been built without the skilled support provided by the technical services of the Research School of Physical Sciences and Engineering. We acknowledge Professor H. Bross for communicating the Gaussian grid for the spherical integration. M.V. was supported by the Australian Research Council and F.A. acknowledges support from NEDO.

[1] N. W. Ashcroft and N. D. Mermin, *Solid State Physics* (Saunders College, 1976).
[2] L. Hedin, Phys. Rev. **139**, A796 (1965).
[3] L. Hedin and S. Lundqvist, in *Solid State Physics*, edited by D. Turnbull and H. Ehrenreich (Academic, New York, 1969), Vol. 23, p. 1.
[4] F. Aryasetiawan and O. Gunnarsson, Rep. Prog. Phys. **61**, 237 (1998).
[5] D. Langreth, Phys. Rev. B **1**, 471 (1970).
[6] B. Bergersen, F.W. Kus, and C. Blomberg, Can. J. Phys. **51**, 102 (1973).
[7] L. Hedin, Phys. Scr. **21**, 477 (1980).
[8] F. Aryasetiawan, L. Hedin, and K. Karlsson, Phys. Rev. Lett. **77**, 2268 (1996).
[9] M. Vos, A. Kheifets, E. Weigold, S. Canney, B. Holm, F. Aryasetiawan, and K. Karlsson, J. Phys.: Condens. Matter **11**, 3645 (1999).
[10] P. Steiner, H. Höchst, and S. Hüfner, in *Photoemission in Solids II* (Springer-Verlag, Berlin, 1978), p. 349.
[11] L. Levinson, F. Greuter, and E. Plummer, Phys. Rev. B **27**, 727 (1983).
[12] C. Heske, R. Treusch, F. Himpsel, S. Kakar, L. Terminello, H. Weyer, and E. Shirley, Phys. Rev. B **59**, 4680 (1999).
[13] M. Cooper, Rep. Prog. Phys. **48**, 415 (1985).
[14] F. Kurp, M. Vos, T. Tschentscher, A. Kheifets, E. Weigold, J. Schneider, and F. Bell, Phys. Rev. B **55**, 5440 (1997).
[15] W. Schülke, G. Stutz, F. Wohlert, and A. Kaprolat, Phys. Rev. B **54**, 14 381 (1996).
[16] Suortti *et al.*, J. Phys. Chem. Solids **61**, 397 (2000).
[17] M. Vos and I. McCarthy, Rev. Mod. Phys. **67**, 713 (1995).
[18] V. Neudatchin, Y.V. Popov, and Y.F. Smirnov, Phys. Usp. **42**, 1017 (1999).
[19] E. Weigold and I. McCarthy, *Electron Momentum Spectroscopy* (Kluwer Academic/Plenum, New York, 1999).
[20] M. Vos, G. Cornish, and E. Weigold, Rev. Sci. Instrum. **71**, 3831 (2000).
[21] M. Vos and E. Weigold, J. Electron Spectrosc. Relat. Phenom. **112**, 93 (2000).
[22] A. Kheifets, D. Lun, and S.Y. Savrasov, J. Phys.: Condens. Matter **11**, 6779 (1999).
[23] B. Holm and F. Aryasetiawan, Phys. Rev. B **56**, 12 825 (1997).
[24] W. Fehlner, S. Nickerson, and S. Vosko, Solid State Commun. **19**, 83 (1976).
[25] S. Tanuma, C. Powell, and D. Penn, Surf. Interface Anal. **20**, 77 (1993).
[26] R. Jones and A. Ritter, J. Electron Spectrosc. Relat. Phenom. **40**, 285 (1986).
[27] M. Vos and M. Bottema, Phys. Rev. B **54**, 5946 (1996).